

Circumventing additivity in molecular mechanics with conformationally-dependent surface hopping

Tristan Bereau* and Joseph F. Rudzinski

Max Planck Institute for Polymer Research, 55128 Mainz, Germany

(Dated: June 8, 2022)

Classical molecular dynamics strategies are inherently limited by the molecular-mechanics basis set employed. Here we extend the concept of multisurface dynamics, initially developed to describe electronic transitions in chemical reactions, to sample the conformational ensemble of a classical system in equilibrium. In analogy to describing different electronic configurations, a surface-hopping scheme couples distinct conformational basins. A structural criterion for the surface selection effectively introduces coupling beyond the additivity of the Hamiltonian. We illustrate the method through a systematic coarse-graining of two molecular systems that give rise to notoriously challenging many-body potentials of mean force. Incorporating more surfaces leads systematically towards unimodal distributions within each basin, resulting in structural improvements that also yield kinetic consistency.

Computer simulations of condensed-matter systems have had enormous impact in the last decades, rising as a complementary pillar to experiments and analytical theory [1, 2]. While hardware and algorithmic developments have vastly improved our ability to sample conformational space, the molecular-mechanics functional forms of most simulation studies have remained roughly the same for the last 40 years [3, 4]. Going beyond standard additive force fields can prove extremely beneficial, as demonstrated by recent developments in polarizable models [5]. Unfortunately, expanding the molecular-mechanics basis set often remains computationally prohibitive. Alternative avenues using machine learning show significant promise, but remain challenging for accurate treatment of long-range interactions [6–8]. In this Letter, we present a unique strategy for generating complex cross-correlations between interaction terms of a force field, while retaining the simplicity of the conventional molecular-mechanics basis set.

Limitations of the molecular-mechanics basis set have long been addressed for chemical reactions by methods such as empirical valence bond [9], its multisurface extension [10], and surface-hopping schemes [11]. In these approaches, reactions are effectively decomposed into surfaces with distinct electronic configurations, such as the two bonded states for a proton transfer. The limitations of the basis set are overcome by coupling distinct potential-energy surfaces through surface-hopping dynamics.

In the classical simulation community, researchers have coupled distinct force fields to describe internal-state conversions of coarse-grained units [12], entanglement in polymer melts [13], and large-scale conformational transitions of biomolecules [14]. In the case that the force field interaction functions can be expressed analytically as a function of a continuous order parameter, e.g., in dissipative particle dynamics models with local density-dependent potentials [15], no explicit hopping protocol

is required, as the dynamics along the continuous hypersurface of force fields is well-defined by the normal integration scheme. On the other hand, if switching between force fields is discrete and, in particular, if a timescale separation exists between force field transitions and the local motion of particles, Monte Carlo provides a robust route for instantaneous switching between force fields. Voth and coworkers have recently laid out an elegant “ultra coarse-graining” framework in this context, where conversions between discrete internal states are modeled by stochastic transitions between distinct force fields [16, 17].

In the present work, we expand upon previous efforts by considering the common situation where significant coupling between local degrees of freedom in the simulation model are essential for accurate modeling of the structural ensemble. To address this challenge, we draw an analogy between electronic transitions and transitions between conformational basins, in the context of surface-hopping techniques. Instead of matching the potential-energy surface due to different types of electronic configurations, we aim to reproduce features of distinct conformational basins of the underlying free-energy surface. Thus, we assign distinct force fields to conformations belonging to a given basin, and hop between conformationally-dependent surfaces. Rather than hop between surfaces in a stochastic manner, we ascribe a continuous-switching scheme, motivated by the classical description of the problem. In contrast to previous studies employing discrete transitions between distinct force fields, the transitions between local conformational basins considered in this work occur on comparable timescales to the local dynamics, discouraging the use of the Monte Carlo approaches. Surface-hopping schemes for chemical reactions typically weight each surface according to solutions of the Schrödinger equation, effectively leading to a strong dependence on the relative energies. Because we aim at reproducing the free energy of each conformational basin, we require an integrated measure. As such we define the weights using a structural criterion: a metric depending collec-

* bereau@mpip-mainz.mpg.de

tively on the instantaneous values of the order parameters governing each interaction. Despite retaining the standard molecular-mechanics form of individual force fields, the conformationally-dependent surface hopping generates complex cross-correlations between local degrees of freedom, as we will demonstrate below.

To test the ability of our methodology to recover cross-correlations beyond the additivity limit of standard force fields, we focus on notoriously challenging problems from structure-based coarse-graining (CG) [18–21]. Instead of targeting a potential energy surface, averaging over degrees of freedom leads to a many-body potential of mean force (MB-PMF) [22, 23]. While several systematic methods exist to target the MB-PMF [22, 24–26] their accuracy tends to be limited not by the performance of the method, but rather by the molecular-mechanics basis used to approximate the MB-PMF. Several recent attempts have been made at expanding the basis set [27–29], illustrating the need for more accurate models.

We demonstrate the surface-hopping methodology by coupling several interactions together: bond with bending angle for a three-bead hexane molecule in vacuum, and bending-angle with dihedral for an implicit-solvent, four-bead tetraalanine peptide. By optimizing the potentials over subsets of the conformational ensemble, we show that the method provides a significant increase in structural accuracy compared to state-of-the-art structure-based CG methods. The structural improvements are such that the model recovers kinetic consistency, as measured by its long timescale dynamical properties.

Methodology. The procedure consists of modeling a molecular system by means of n force fields that collectively describe conformational space. Each force field is optimized to reproduce only a subset of conformational space, obtained from a density-based cluster analysis performed on the mean-centered, normalized distributions along the order parameters governing each interaction term in the CG potential [30]. The initial clusters were systematically coarsened to generate representations from 1 to n clusters. Each force field is then built from the relevant sub-trajectories parsed according to cluster identities.

The cluster \mathcal{C}_i aims at coupling a set of k interactions $\zeta_1^{(i)}, \zeta_2^{(i)}, \dots, \zeta_k^{(i)}$ (Fig. 1). We further define the cluster center, $\mu^{(i)} = (\mu_1^{(i)}, \mu_2^{(i)}, \dots, \mu_k^{(i)})$, corresponding to a local maximum of probability density across each variable. Similarly, we define the spatial extent of the cluster by means of its standard deviation, $\sigma^{(i)} = (\sigma_1^{(i)}, \sigma_2^{(i)}, \dots, \sigma_k^{(i)})$. We apply a linear transformation on the clusters to enhance their isotropy: $\bar{\sigma}^{(i)} = (\bar{\sigma}_1^{(i)}, \bar{\sigma}_2^{(i)}, \dots, \bar{\sigma}_k^{(i)})$.

Force field i is characterized by its potential energy, $U_i(\mathbf{R})$, and corresponding force $f_{i,\alpha}(\mathbf{R}) = -\nabla_\alpha U_i(\mathbf{R})$ along component α . Force field i is assigned a coefficient w_i that weights its instantaneous contribution. This contribution depends on the set of k interactions $\{\zeta_j\}_{j=1}^k$ in-

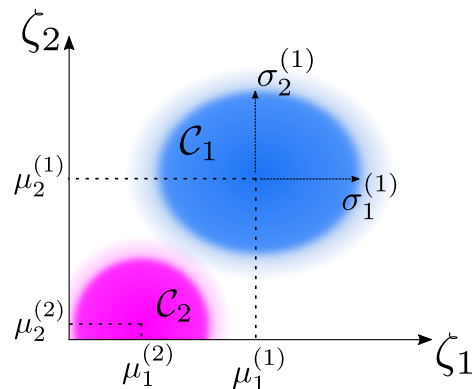


FIG. 1. The conformational space of the system is projected onto the interactions $\{\zeta_i\}$ and subdivided into regions of high density. Each one is identified by a cluster \mathcal{C}_j , with center $\mu^{(i)}$ and size $\sigma^{(i)}$. To each cluster is associated a local force field. The system then hops between force fields—or surfaces. The remaining white region is modeled by a general, fallback force field.

cluded in cluster \mathcal{C}_i , such that $w_i = w_i(\{\zeta_j(\mathbf{R})\}_{j=1}^k)$. The force on any particle is then a weighted sum over all force fields

$$f_\alpha(\mathbf{R}) = \sum_{i=1}^n w_i f_{i,\alpha}(\mathbf{R}). \quad (1)$$

The weight w_i of force field i is determined by the distance of the instantaneous collective variable, $z = (z_1, z_2, \dots, z_k)$, to the center of cluster \mathcal{C}_i

$$d^2(z, \mu^{(i)}) = \sum_{j=1}^k \left(\frac{z_j - \mu_j^{(i)}}{\bar{\sigma}_j^{(i)}} \right)^2, \quad (2)$$

where the scaling by $\bar{\sigma}_j$ normalizes the contribution of each interaction. This distance is compared to the spatial extent of cluster \mathcal{C}_i , defined from the L2-norm $|\bar{\sigma}^{(i)}|$. The weight is defined as

$$w_i = \begin{cases} 1, & d(z, \mu^{(i)}) < |\bar{\sigma}^{(i)}| \\ \exp\left(-\frac{d(z, \mu^{(i)}) - |\bar{\sigma}^{(i)}|}{\alpha}\right), & \text{otherwise.} \end{cases} \quad (3)$$

The scaling factor α smoothly dampens the contribution of force field i to avoid numerical instabilities upon integrating the equations of motion. A value of α that is small compared to the spatial extent of any cluster center avoids the blurring of the different potential energy surfaces.

The mixing of several force fields, as described in Eqn. 1, can easily lead to unphysical behavior, even from a weak contribution of a surface containing large restoring forces. To avoid such a behavior, we restrict the mixing as much as possible. This is achieved by defining the first $n - 1$ surfaces that are localized to a cluster

center, while the last force field n embodies the default option. This fallback surface is thus *not* associated to any cluster center, but instead parametrized from the rest of the trajectory that has not yet been considered. We compute the weights w_i (Eqn. 3) for the first $n - 1$ surfaces, keep only the one with the largest contribution $w_l = \max_{i < n} w_i$, and assign the rest of the weight to the fallback surface, $w_n = 1 - w_l$. As such, the surface mixing described in Eqn. 1 is always limited to the closest cluster center and the fallback force field. When the system is far from any cluster center, it relies solely on the fallback surface ($w_n = 1$). Our scheme directly hops between surfaces without rescaling velocities, and thereby violates total-energy conservation. In the canonical ensemble the thermostat is capable of absorbing a certain amount of energy violation [17], which we enhance by working at high friction.

While the algorithm described above yields surface hopping, it doesn't ensure the correct probabilities of sampling each surface. To this end, the ultra coarse-graining framework matches the transition rates through a self-consistent optimization [17]. Here we simply enforce the system to sample each surface i such that the time average $\langle w_i \rangle$, taken as a proxy of its canonical probability, matches the target probability p_i —available upon partitioning of the conformational space. The matching is enforced by locking the system that is currently visiting surface i on that force field until $\langle w_i \rangle \approx p_i$. In practice, we let the system escape from surface i once $\langle w_i \rangle \geq 0.98 p_i$. While we only constrain a lower bound on sampling each surface, our experience so far indicates that it is sufficient to recover the right probabilities.

All simulation details are described in the Supporting Information (SI). An ESPRESSO++ [31] implementation of the surface-hopping scheme is available online [32], as well as all simulation and analysis scripts [33].

Hexane. We first consider a 3-site representation for hexane, which represents subsequent pairs of carbon atoms with a CG site. The CG potential employed bonded interactions between subsequent pairs of sites along the chain and an angle-bending interaction between the three CG sites. This CG model was first described in Rühle *et al.* [34]. The force-matching-based multiscale coarse-graining (MS-CG) method applied to the reference atomistic (AA) trajectory led to significant structural discrepancies, as seen in the 1-dimensional bending-angle distribution (Fig. 2b). MS-CG overpopulates small-angle states ($100^\circ < \theta < 120^\circ$), while underpopulating the high-angle states ($\theta > 150^\circ$). Rudzinski and Noid later demonstrated that these discrepancies arise due to bond-angle cross-correlations that cannot be reproduced with the molecular-mechanics interaction set [35]. They applied an iterative generalized Yvon-Born-Green (iter-gYBG) scheme to reproduce the independent bond and bending-angle reference AA distributions, albeit at the cost of accuracy in the cross-correlations. The discrepancies in the cross-correlations between bond and bending angle generated by these

models is illustrated by the free-energy surfaces (FES) in Fig. 3. The AA model displays a complex surface made of four major minima, located asymmetrically on the surface. The symmetry of the iter-gYBG model, on the other hand, clearly illustrates the additivity of the interactions in the Hamiltonian: all large-bond states are more populated than the small-bond states, irrespective of the angle.

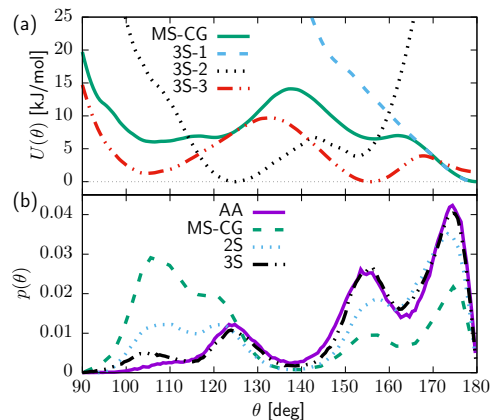


FIG. 2. Bending-angle properties of the CG hexane molecule. (a) Potential energy from force matching (MS-CG) and the three contributions of the 3-surface (3S) model. (b) Probability distribution from the atomistic distribution projected onto CG variables (AA), force matching (MS-CG), and surface hopping with 2 (2S) and 3 (3S) force fields.

A clustering of conformational space in two surfaces (i.e., 2S model) leads to: (2S-1) the highest angle state coupling to the large bond state (cluster center: $b = 0.26$ nm, $\theta = 170^\circ$) and the fallback surface (2S-2). Fig. 2a shows how a 3-state CG model discriminates between: (3S-1) the highest angle state—identical to 2S-1; (3S-2) two intermediate angles ($\theta \approx 125^\circ$, $\theta \approx 155^\circ$) with large bond; and the fallback surface (3S-3): an intermediate and a low angle state ($\theta \approx 155^\circ$, $\theta \approx 105^\circ$) around both small and large bond states.

Fig. 2b displays the bending-angle canonical distributions for the different CG models. We find that 2S and 3S systematically refine the agreement with the AA distribution as compared to MS-CG: they lower the artificially large populations of small-angle states and increase the artificially-low populations of high-angle states. The 3S model reproduces the AA angle distribution remarkably accurately, with only a slightly-low population around $\theta \approx 105^\circ$. In addition, the interaction potentials become more localized: while the MS-CG potential is extremely broad, the different 3S potentials are better confined.

The effect of the surface hopping technique is even more apparent in the FES. The 2S model demonstrates significant improvement relative to the standard

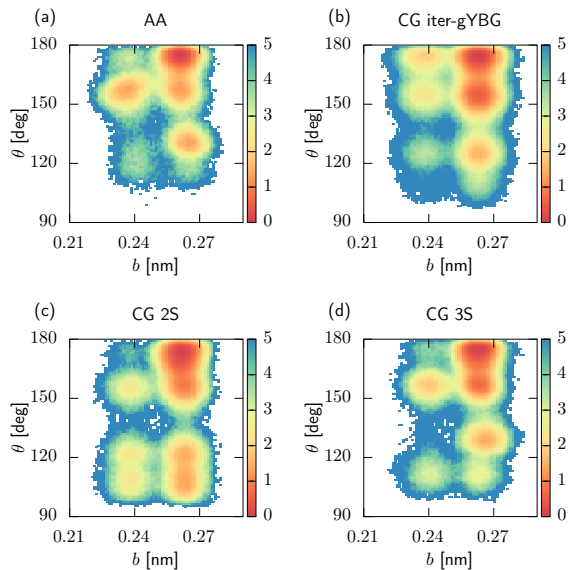


FIG. 3. Free-energy surfaces of the hexane molecule as a function of the bond, b , and bending angle, θ . (a) Reference surface; (b) CG iterative gYBG, (c) CG 2-state and (d) CG 3-state surfaces. Free energies expressed in $k_B T$.

molecular-mechanics force field by more accurately representing the heterogeneous populations of high-angle states. The 3S model further corrects the populations, especially for the low-angle states.

Tetraalanine: As a second system, we consider an implicit-solvent, 1-site-per-amino-acid representation for Ala₄ [36]. Each bead was placed at the position of the alpha carbon on the peptide backbone. The CG force field employed bonded interactions between subsequent pairs of sites along the peptide chain, two angle-bending interactions, a dihedral interaction, ψ , and an additional effective bond between the terminal beads of the chain, R_{1-4} .

Both MS-CG and iter-gYBG models displayed two notable discrepancies on the FES (Fig. 4 and SI): a spurious region of intermediates ($\psi \approx 90^\circ$, $R_{1-4} \approx 0.9$ nm) and the extended state stabilized at too large dihedrals ($\psi \approx -90^\circ$, $R_{1-4} \approx 0.6$ nm). Surface-hopping models with 2 and 3 surfaces suppress both regions. Further, a 4S model (SI) shows structural accuracy on par with 3S.

Beyond structural properties, the dynamics also show significant improvements. We monitor the transition kinetics between the helical (H) and extended (E) metastable basins (Fig. 5a), identified from a Markov state model analysis [37, 38] of the reference AA simulation [36, 39]. We focus on *ratios* of mean-first-passage times to factor out any homogeneous speedup factor due to coarse-graining. While the MS-CG and iter-gYBG models display serious discrepancies, the surface hopping schemes are significantly closer to the AA result (Fig. 5b). We observe a systematic improvement as a function of

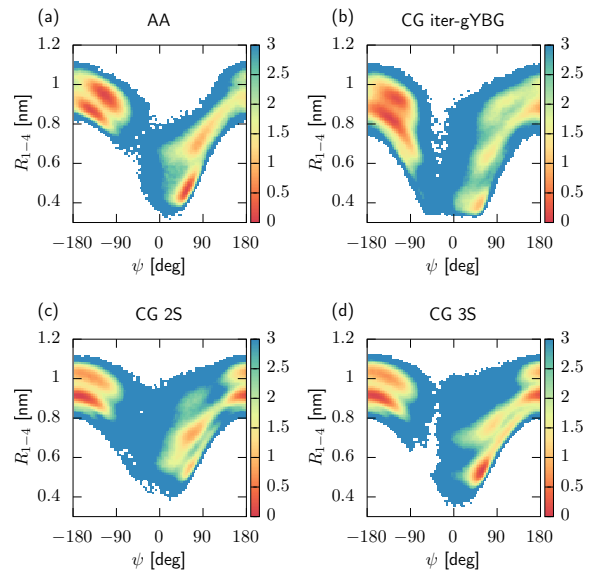


FIG. 4. Free-energy surfaces of Ala₄ as a function of the dihedral, ψ , and end-to-end distance, R_{1-4} . (a) Reference surface; (b) CG iterative gYBG, (c) CG 2-state and (d) CG 3-state surfaces. Free energies expressed in $k_B T$.

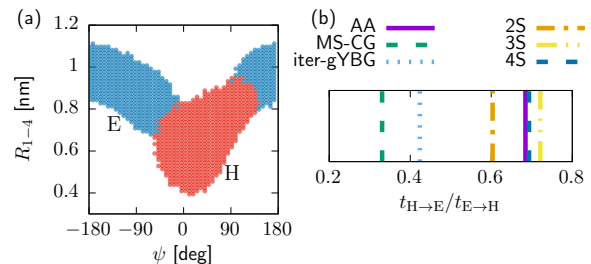


FIG. 5. (a) Basin decomposition between helical (H) and extended (E) states. (b) Ratio of mean-first-passage times between the helical and extended states, $t_{H \rightarrow E}/t_{E \rightarrow H}$.

the number of surfaces, where 4S reproduces the reference AA observable virtually quantitatively. Division of the MB-PMF into distinct regions results in a simplification of the individual target structures that can be more accurately described with a conventional molecular mechanics force field. As a consequence, the surface-hopping technique not only improves the description of the basin minima, but also the free-energy barriers between basins and, thus, also the slow kinetic processes, up to an arbitrary speedup factor [40].

The systems considered in this work highlight the capability of the surface-hopping scheme: to introduce cross-correlations between interaction terms beyond the additivity assumption of the Hamiltonian. Our results demonstrate improved structural and kinetic accuracy for CG models beyond state-of-the-art techniques. This improvement is due not only to the introduction of cross-

correlations between interactions, but also to the simplification of the target surface when determining each force field. In particular, we have found that as the number of surfaces increases, the distributions within each basin become increasingly unimodal, resulting in very simple interaction potentials and systematically improving the accuracy of the model. Alternative strategies to our method could include: a potential expressed as the product of multiple interactions or a new interaction acting as a proxy for the cross-correlations between existing terms. While the former would likely require significant reference sampling, identifying suitable candidates makes the latter approach challenging. Furthermore, the flexibility of coupling any set of interactions makes our approach amenable to scaling up to larger systems. Beyond

our results, we expect the accurate description of cross-correlations between interaction terms to have broad impact for condensed-matter modeling across scales.

ACKNOWLEDGMENTS

We thank Denis Andrienko, Kurt Kremer, and Clemens Rauer for insightful discussions. This work was supported in part by the TRR 146 Collaborative Research Center of the Deutsche Forschungsgemeinschaft (DFG), the Emmy Noether program to TB and a post-doctoral fellowship from the Alexander von Humboldt foundation to JFR.

-
- [1] M. Ferrario, G. Ciccotti, and K. Binder (eds), *Computer simulations in condensed matter: from materials to chemical biology*, Vol. 1 (Springer, 2007).
- [2] S. Bottaro and K. Lindorff-Larsen, *Science* **361**, 355 (2018).
- [3] M. Karplus and D. L. Weaver, *Nature* **260**, 404 (1976).
- [4] S. Piana, J. L. Klepeis, and D. E. Shaw, *Current opinion in structural biology* **24**, 98 (2014).
- [5] J. W. Ponder, C. Wu, P. Ren, V. S. Pande, J. D. Chodera, M. J. Schnieders, I. Haque, D. L. Mobley, D. S. Lambrecht, R. A. DiStasio Jr, *et al.*, *The journal of physical chemistry B* **114**, 2549 (2010).
- [6] A. P. Bartók, M. C. Payne, R. Kondor, and G. Csányi, *Physical review letters* **104**, 136403 (2010).
- [7] S. Chmiela, A. Tkatchenko, H. E. Sauceda, I. Poltavsky, K. T. Schütt, and K.-R. Müller, *Science advances* **3**, e1603015 (2017).
- [8] T. Bereau, R. A. DiStasio Jr, A. Tkatchenko, and O. A. Von Lilienfeld, *The Journal of Chemical Physics* **148**, 241706 (2018).
- [9] A. Warshel and R. M. Weiss, *Journal of the American Chemical Society* **102**, 6218 (1980).
- [10] U. W. Schmitt and G. A. Voth, *The Journal of Physical Chemistry B* **102**, 5547 (1998).
- [11] J. C. Tully, *The Journal of Chemical Physics* **93**, 1061 (1990).
- [12] T. Murtola, M. Karttunen, and I. Vattulainen, *J. Chem. Phys.* **131**, 55101 (2009).
- [13] V. C. Chappa, D. C. Morse, A. Zippelius, and M. Müller, *Physical Review Letters* **109**, 1 (2012).
- [14] M. Knott and R. B. Best, *The Journal of chemical physics* **140**, 05B603.1 (2014).
- [15] I. Pagonabarraga and D. Frenkel, *The Journal of Chemical Physics* **115**, 5015 (2001).
- [16] J. F. Dama, A. V. Sinitskiy, M. McCullagh, J. Weare, B. Roux, A. R. Dinner, and G. A. Voth, *Journal of chemical theory and computation* **9**, 2466 (2013).
- [17] A. Davtyan, J. F. Dama, A. V. Sinitskiy, and G. A. Voth, *Journal of chemical theory and computation* **10**, 5265 (2014).
- [18] T. Murtola, A. Bunker, I. Vattulainen, M. Deserno, and M. Karttunen, *Physical Chemistry Chemical Physics* **11**, 1869 (2009).
- [19] C. Peter and K. Kremer, *Soft Matter* **5**, 4357 (2009).
- [20] C. Peter and K. Kremer, *Faraday discussions* **144**, 9 (2010).
- [21] S. C. Kamerlin, S. Vicatos, A. Dryga, and A. Warshel, *Annual review of physical chemistry* **62**, 41 (2011).
- [22] W. Noid, J.-W. Chu, G. S. Ayton, V. Krishna, S. Izvekov, G. A. Voth, A. Das, and H. C. Andersen, *The Journal of chemical physics* **128**, 244114 (2008).
- [23] J. F. Rudzinski and W. Noid, *The Journal of chemical physics* **135**, 214101 (2011).
- [24] W. Tschöp, K. Kremer, J. Batoulis, T. Bürger, and O. Hahn, *Acta Polymerica* **49**, 61 (1998).
- [25] W. Noid, P. Liu, Y. Wang, J.-W. Chu, G. S. Ayton, S. Izvekov, H. C. Andersen, and G. A. Voth, *The Journal of chemical physics* **128**, 244115 (2008).
- [26] M. S. Shell, *The Journal of chemical physics* **129**, 144108 (2008).
- [27] V. Molinero and E. B. Moore, *The Journal of Physical Chemistry B* **113**, 4008 (2008).
- [28] T. Sanyal and M. S. Shell, *The Journal of Physical Chemistry B* **122**, 5678 (2018).
- [29] S. T. John and G. Csányi, *The Journal of Physical Chemistry B* **121**, 10934 (2017).
- [30] F. Sittel and G. Stock, *Journal of chemical theory and computation* **12**, 2426 (2016).
- [31] J. D. Halverson, T. Brandes, O. Lenz, A. Arnold, S. Bevc, V. Starchenko, K. Kremer, T. Stuehn, and D. Reith, *Computer Physics Communications* **184**, 1129 (2013).
- [32] <https://github.com/tbereau/espressopp>, accessed August 1, 2018.
- [33] https://gitlab.mpcdf.mpg.de/trisb/cg_surf_hop, accessed August 1, 2018.
- [34] V. Rühle, C. Junghans, A. Lukyanov, K. Kremer, and D. Andrienko, *Journal of Chemical Theory and Computation* **5**, 3211 (2009).
- [35] J. F. Rudzinski and W. G. Noid, *Journal of Physical Chemistry B* **118**, 8295 (2014).
- [36] J. F. Rudzinski and W. G. Noid, *Journal of Chemical Theory and Computation* **11**, 1278 (2015).
- [37] F. Noé, *J. Comp. Phys.* **28**, 244103 (2008).
- [38] G. R. Bowman, V. S. Pande, and F. Noé, *An Introduction to Markov State Models and Their Application to Long Timescale Molecular Simulation* (Springer Science

- and Business Media, Dordrecht, Netherlands, 2014).
- [39] J. F. Rudzinski, K. Kremer, and T. Berau, The Journal of Chemical Physics **144**, 051102 (2016).
- [40] J. F. Rudzinski and T. Berau, The European Physical Journal Special Topics **225**, 1373 (2016).